Reflection of sound by glow discharge plasma

2006 J. Phys. D: Appl. Phys. 39 3653

(http://iopscience.iop.org/0022-3727/39/16/019)

INSTITUTE OF PHYSICS PUBLISHING JOURNAL OF PHYSICS D: APPLIED PHYSICS

J. Phys. D: Appl. Phys. **39** (2006) 3653–3658 doi:10.1088/0022-3727/39/16/019

Reflection of sound by glow discharge plasma

Vladimir Soukhomlinov[1], **Valery A Sheverev**[2] **and Calin Tarau**[2]

[1]Research Institute for Physics, Saint-Petersburg State University, Saint-Petersburg, Russia
[2]Polytechnic University, Six Metrotech Center, Brooklyn, NY 11201, USA

Received 25 April 2006, in final form 26 April 2006
Published 4 August 2006
Online at stacks.iop.org/JPhysD/39/3653

Abstract
The propagation of sound through temperature gradient regions of a glow discharge plasma is analysed. Using a JWKB solution known for a Schrödinger's equation describing the propagation of quantum particle through a potential barrier, an algorithm for evaluation of the reflection coefficient is proposed. The analytical results are compared with those obtained by numerically solving Euler's equations using a second order finite difference approach. The sound reflection coefficients calculated for temperature distribution profiles that are typical for atmospheric glow discharge plasma demonstrate that, at zero-incidence angle, a significant part, up to 25%, of the wave energy can be reflected. These results indicate that sound attenuation by the atmospheric glow discharge plasma by more than 10 dB, as demonstrated in a recent experiment, can be explained, accounting for three-dimensional effects, by the thermal gradient sound–plasma interaction mechanisms.

1. Introduction

Experimental observations of structural changes in shock waves interacting with a glow discharge [1–4] have generated considerable discussion in the aerospace community. Gas temperature gradients around the plasma formation are believed to be the primary cause for the observed wave modifications [5,6] although certain inherent plasma mechanisms have also been considered for their explanation [7]. Recently, research into the application of glow discharge plasma has been expanded from shock wave mitigation to air vehicle drag reduction [8] and flow control [9, 10]. The present work explores another potential use of plasma: the control of aeroacoustics, particularly, the containment of aircraft noise [11].

In a weakly ionized gas, the evolution of a flow disturbance is affected by the non-uniform temperature field that results in refraction index gradients around the plasma region. A portion of the wave is reflected in these gradient zones and the forward moving wave passing through the plasma is attenuated. Similar effects are observed for other types of disturbances such as shock waves. In fact, the global temperature gradient model was sufficient to explain the changes in the structure of a normal shock wave travelling in a discharge tube [6].

Sound reflection from a boundary separating two uniform media with different temperatures has been investigated in the past for two limiting cases: when the length of the non-uniform zone, Δ, separating the two uniform media, is significantly smaller or larger than the sound wavelength, λ. The first case of $\Delta \ll \lambda$ is described by the two-layer approximation (see, for example [12]) and the opposite limit, $\Delta \gg \lambda$, is a case of a weak non-uniformity that provides an infinitesimally small reflection coefficient that can be neglected in most cases. The intermediate situation of $\Delta \approx \lambda$ has not been studied systematically although several specific aspects of the problem were discussed in [13]. For a typical glow discharge in air at pressures above 50 Torr and discharge current densities of $\sim$10 mA cm^{-2}, the length of the temperature gradient region is several centimetres [14, 15]; thus in the acoustic wave interaction with glow discharge plasma, $\Delta \approx \lambda$. This paper presents the results of an analytical and numerical study of sound wave propagation through a non-uniform gas for an arbitrary value of Δ/λ.

2. Reflection of sound by a non-uniform medium

A one-dimensional equation describing propagation of an acoustic wave in non-uniform medium,

$$\frac{\partial^2 u}{\partial t^2} = a_0^2(x)\frac{\partial^2 u}{\partial x^2}, \tag{1}$$

where $a_0(x)$ is the speed of sound distribution in the undisturbed medium and $u(x,t)$ is the local mass velocity, is known(see, for example, [16]). The equation was obtained by linearizing Euler's equations with respect to the parameter disturbance amplitude and therefore is applicable only for weak acoustic waves. In certain applications, such as mitigation of aircraft noise, modelling of sound with waves of infinitesimally small amplitudes may be insufficient. An alternative approach that allows for accounting of linear and higher-degree terms and that could be used to obtain propagation equations for stronger waves is described in the appendix.

For practical applications, the amount of energy that is reflected by a barrier is of interest. Explicit reflection and transmission coefficients are also required for theoretical and numerical evaluation of the plasma barrier efficiency and optimization. To evaluate the reflection coefficient for a plasma barrier characterized by a temperature distribution $a_0(x)$, we note that equation (1) is identical to the one-dimensional Schrödinger's equation that describes the motion of the quantum particle in a potential field [17]:

$$\frac{\mathrm{d}^2\Phi_0}{\mathrm{d}\xi^2} + \frac{1}{A_0^2}\Phi_0 = 0. \tag{2}$$

Here the mass velocity amplitude $\Phi_0(\xi)$ is defined as $u(\xi,\tau) = \Phi_0(\xi)\mathrm{e}^{i\tau}$ where $\xi = k_0 x$ and $\tau = \omega_0 t$ are the dimensionless coordinate and time, respectively, and $A_0(\xi) = (a_0(\xi/k_0)/A)$ is the normalized speed of sound ($\lim_{\xi\to-\infty} A_0(\xi) = 1$). $A = \lim_{x\to-\infty} a_0(x)$. If the circular frequency of the wave is ω_0 with a corresponding wavelength of λ_0, than $A = (\omega_0/k_0)$ where $k_0 = (2\pi/\lambda_0)$ is the wave number.

A solution to equation (2) can be obtained using the JWKB approximation [17]. For example, Hect and Mayer [18] developed an iteration scheme, which converges well for arbitrary 'smooth' functions $A_0^2(\xi)$, i.e. for mild temperature gradients. This restriction is not applicable to plasma barriers that are characterized by intermediate and sharp gradients. The problem however may be simplified if we restrict our interest to the scattering coefficients.

Following the JWKB approach and introducing variables $\varphi(\xi)$ and $\omega(\xi)$ defined as $\Phi_0(\xi) = g^{-1/2}(\xi)\varphi(\xi)$ and $\omega(\xi) = \int_{\xi_0}^{\xi} g(\xi')\mathrm{d}\xi'$ where $g(\xi)$ is a certain function and ξ_0 is an arbitrary constant, equation (2) may be rewritten as

$$\frac{\mathrm{d}^2\varphi}{\mathrm{d}\omega^2} + (1+\varepsilon)\varphi = 0, \tag{3}$$

where

$$\varepsilon = \frac{\frac{1}{A_0^2} - g^2}{g^2} - g^{-1/2}\frac{d^2(g^{1/2})}{\mathrm{d}\omega^2} = \frac{\frac{1}{A_0^2} - g^2}{g^2} + g^{-3/2}\frac{\mathrm{d}^2(g^{-1/2})}{\mathrm{d}\xi^2}.$$

The reflection coefficient then, in the JWKB limits, is expressed in terms of the following integrals [16]:

$$\mu = \int_0^{\omega} \varepsilon(\omega')\mathrm{d}\omega',$$
$$K_0 = i\int_{x'-iy'}^{x'+iy'} g(z)\mathrm{d}z,\ y' > 0, \tag{4}$$

where $x' \pm iy'$ are the closest to the real axis roots of equation $g(z) = 0$. Using the connection between $\omega(z)$ and $g(z)$: $(\mathrm{d}\omega/\mathrm{d}z) = g(z)$, the first of the two integrals can be approximated with

$$\mu \approx -\frac{1}{4}\int_L \frac{1}{A_0(\xi)}\left[\frac{\mathrm{d}A_0(\xi)}{\mathrm{d}\xi}\right]^2 \mathrm{d}\xi. \tag{5}$$

Here the integration is performed over the length of the gradient zone, L. Reflection coefficient K_0 does not depend on x'. This coordinate defines only the position of the potential barrier [17]. The value of y' is affected by the maximum value of the function $(1/A_0(\xi))$ and the magnitude of its derivative at the location of the function maximum. In summary, the reflection coefficient is determined not so much by the specific shape of the potential barrier, but by its characteristic length and height, which are expressed by integrals μ and K_0 .The reflection coefficient is not therefore as sensitive to the actual shape of temperature profile $T(\xi)$ as to the ratio of $(T_{\max}/T(-\infty))$ (or $(T_{\min}/T(-\infty))$) and the length of the gradient zone.

The above consideration leads to the following algorithm for the approximation of the reflection coefficient. A solution for Schrödinger's equation (2) is known for the potential (or, in sound propagation terms, temperature) barrier that is given by

$$\frac{T}{T_0} = \frac{B^2(1+\mathrm{e}^{-\alpha\xi})}{1+B^2\mathrm{e}^{-\alpha\xi}} = \frac{B^2(1+\mathrm{e}^{-\beta x})}{1+B^2\mathrm{e}^{-\beta x}}, \tag{6}$$

where α and B are arbitrary constants and $\beta = k_0\alpha$. For this distribution, the reflection coefficient is [16]

$$R = \left\{\frac{\mathrm{sh}\left[\frac{\pi}{\alpha}\left(1-\frac{1}{B}\right)\right]}{\mathrm{sh}\left[\frac{\pi}{\alpha}\left(1+\frac{1}{B}\right)\right]}\right\}^2. \tag{7}$$

Here the speed of sound changes by a factor of B over the domain $-\infty < \xi < \infty$, while $(1/\beta)$ represents the characteristic length of the temperature gradient region. It follows from (7) that the reflected wave vanishes in a uniform medium or at very mild temperature gradients (i.e. $R \to 0$ as $B \to 0$ or $\alpha \to 0$). When $\alpha \to \infty$, the temperature profile is a step-function, and $R = ((B-1)/(B+1))^2$.

This result was first obtained by Strutt [12].

To calculate the best approximation for the reflection coefficient, the actual temperature profile should be appropriately approximated by distribution (6). The fitting requirement here is the match of the scattering integrals (4) for the experimental temperature distribution and the model function (6), respectively. Specifically, the algorithm is (1) integrals μ and K_o are calculated for the actual distribution; next, by evaluating model distribution (6), (2) the values of B and β are obtained that would result in the same values of μ and K_o as those calculated for the actual distribution and (3) the sound reflection coefficient is then calculated using equation (7). Note that the best-fit model function obtained according to this criterion may locally be noticeably different from the actual distribution.

Using the JWKB approximation, a condition for the 'smoothness' of the potential barrier required for the reflection coefficient to be infinitesimally small can be obtained [17]:

$$\frac{1}{4\pi}\frac{a_0(x)}{A}\left|\frac{\Delta_\lambda\left(\frac{\mathrm{d}a_0}{\mathrm{d}x}\right)}{\frac{\mathrm{d}a_0}{\mathrm{d}x}} - \frac{\Delta_\lambda a_0(x)}{a_0(x)}\right| \ll 1, \tag{8}$$

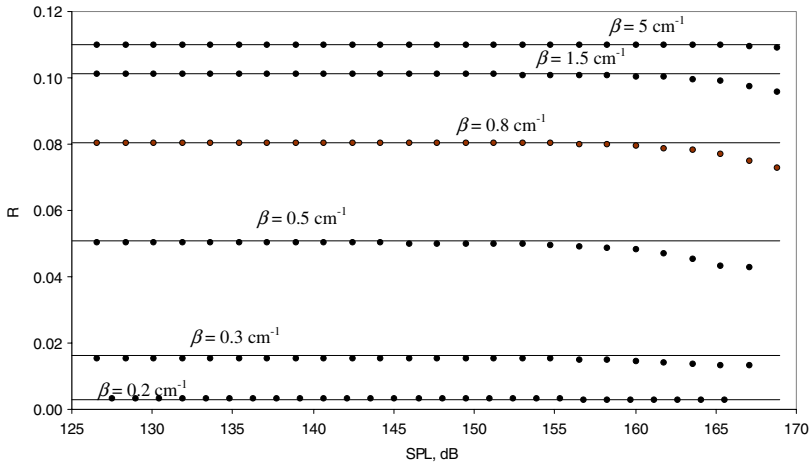

Figure 1. Reflection coefficient versus SPL. Temperature distributions are given by equation (23) with $B = 2$. Wave frequency is 1 kHz. Solid circles are the numerical solutions to the Euler's equations; solid lines represent analytical solutions given by (22).

where Δ_λ is the change of the value over the acoustic wavelength. For a typical glow discharge in air at pressures of tens of Torr, the characteristic length of the temperature gradient region is of the order of several centimetres [14]. For this length of the barrier, sound reflection is small for acoustic wave frequencies $\nu_0 \gg 10$ kHz, whereas for $\nu_0 \ll 1$ kHz, the two-layer approximation (with a stepwise temperature jump) is sufficient to evaluate the magnitude of the reflection coefficient.

3. Numerical approach

The propagation of the sound wave through a gas with non-uniform temperature distribution was studied also by solving Euler's equations numerically. A second-order accurate finite-difference scheme with a two-step predictor–corrector discretization was used [19]. The calculation domain consisted of two regions with uniform gas properties but with different temperatures separated by a third region where the temperature was changing between these two values as an arbitrary function of x. In the absence of the wave, the pressure was uniform throughout the domain. The sound wave was introduced as part of the initial conditions at a certain distance upstream of the temperature gradient zone as a sinusoidal variation in pressure, with the corresponding variation in temperature, density and mass velocity superimposed on the uniform gas. The frequency, amplitude and the length (number of cycles) of the initial sound wave were parameters of the problem. An average number of 5712 nodes were used although this number varied slightly as the relative length of the temperature gradient zone was varied.

4. Results

Numerically calculated reflection coefficients for a 1 kHz acoustic wave are compared in figure 1 with those given by equation (7), at various sound pressure levels (SPL) for a range of temperature gradients. The temperature profiles were modelled by (6) using a fixed value of $B = 2$ while varying β. The analytical and numerical solutions agree in figure 1 for the entire range of parameter β in the linear wave domain (SPL < 160 dB) but they tend to diverge at higher amplitudes of the wave. Figure 2 helps explain the smaller values of the numerically calculated reflection coefficients at higher SPL. This figure shows the dependence of the reflection coefficient on sound frequency for a linear wave (SPL $= 150$ dB). For a given β, the higher the sound frequency is, the lower is the reflection coefficient. As the SPL are increased and the wave becomes non-linear (SPL < 160 dB in figure 1), the single-tone wave pattern is distorted and high frequency tones are introduced. These higher frequency components of the non-linear waves in figure 1 are not reflected as efficiently as the base frequency is, thus reducing the total reflected energy of the wave and thus the overall reflection coefficient. Figure 3 compares the numerically and analytically calculated reflection coefficients for a linear wave at various temperature ratios between the two uniform gas regions. The reflection coefficient is a strong function of the temperature ratio and the temperature gradient length. As much as 25% of the incoming wave can be reflected if $B > 3$ (the temperature ratio is nine) at relatively mild ($\beta \sim 1\ \mathrm{cm}^{-1}$) gradients. As follows from figures 1–3, the numerical and analytical solutions agree well for a wide range of parameters ω, B and β. A slight disagreement observed at lower frequencies for mild gradients (for β smaller than $0.8\ \mathrm{cm}^{-1}$ in figure 2) can be attributed to the numerical dissipation in the computational results.

Figure 4 represents the reflection coefficients for a sound wave propagating through the boundary between air and glow discharge plasma, calculated for the plasma parameters of a recent experiment [11] where the attenuation of acoustic waves by a glow discharge plasma in air at a gas pressure of 80 Torr and discharge current densities between 10 and $50\ \mathrm{mAcm}^{-1}$ was studied. Since the gas temperature was not measured in the experiment, the 'actual' temperature profiles are calculated numerically using a model developed in [14]. The calculated profiles (shown with symbols in figure 5) were used to compute scattering integrals K_0 and μ, (4). The model temperature profiles that have the same values of K_0 and μ as the actual distributions are shown with a darker line in figure 5. The corresponding reflection coefficients are denoted similarly in figure 4. The symbols in figure 4 represent the reflection coefficients calculated numerically using actual temperature profiles.

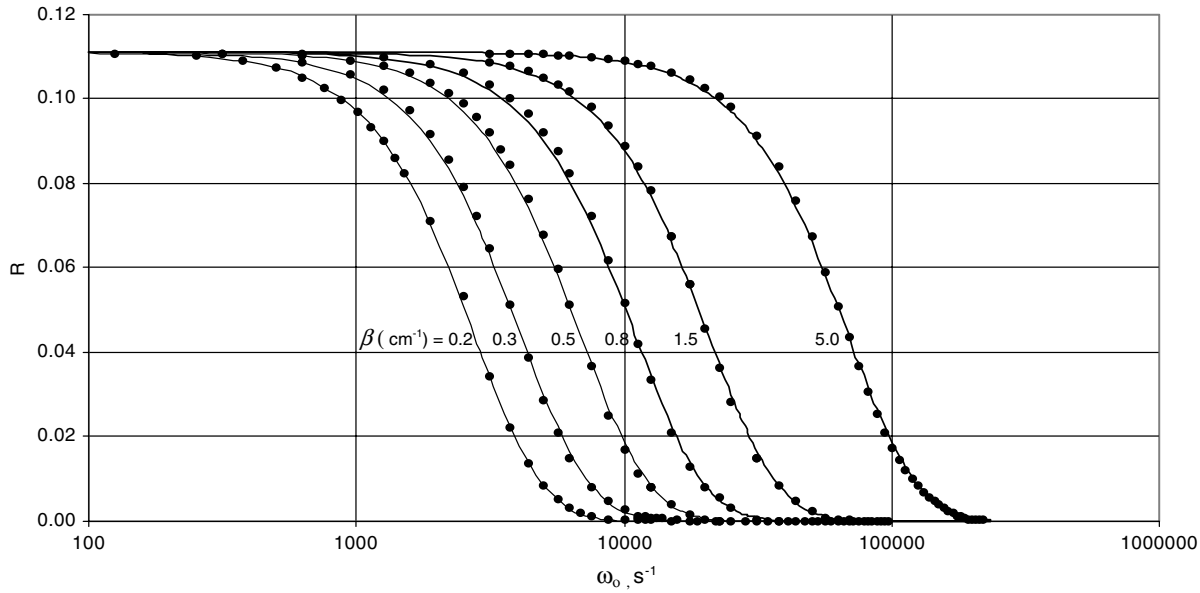

Figure 2. Reflection coefficient versus wave frequency, for $B = 2$. Notation is the same as in figure 1.

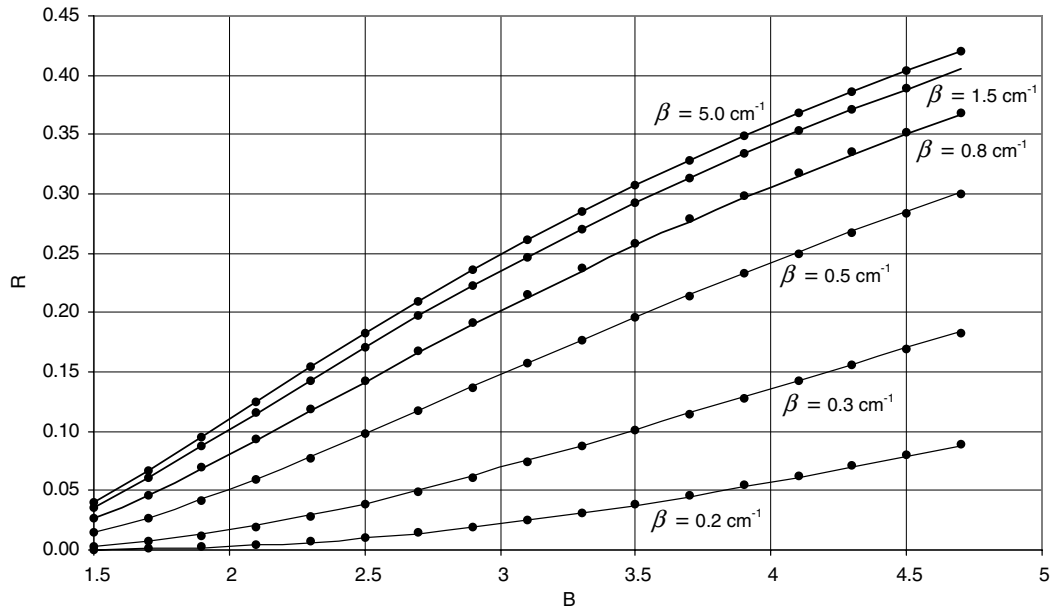

Figure 3. Reflection coefficient versus temperature ratio for the wave frequency 1 kHz. Notation is same as in figure 1.

The scattering integrals approach is compared in figures 4 and 5 to an approximation of the actual temperature distributions with model function (6) using the conventional least-square technique. Parameter B was considered known since it represents the temperature ratio on the boundaries, and only β was evaluated. The model temperature profiles and related reflection coefficients are shown with a lighter line in figures 4 and 5. While the least-square approximation seems to provide a better fit for the actual temperature distributions, the resultant reflection coefficients are not as accurate as those obtained using the scattering integrals algorithm.

It may be observed from figure 4 that the increase in the reflection coefficient due to higher gas temperatures in the plasma (with higher discharge currents) overcomes the decrease in the reflection coefficient due to the expansion of the temperature gradient zone. Overall, the calculations demonstrate that the plasma can significantly reflect acoustic waves for frequencies below 10 kHz. Note that the present analysis is one-dimensional and hence the acoustic wave is incident upon the plasma boundary at zero incidence angle. We also note that the depth of the plasma region, or distance between two plasma boundaries in an experiment, should be comparable to the wavelength, i.e. of the order of ten centimetres, for significant sound reflection. Implementation of such a device may present certain technical challenges. Attenuation of a 13.5 kHz spherical acoustic wave by a glow discharge plasma in air at a gas pressure of 80 Torr and discharge current densities between 10 and 50 mA cm^{-2} was studied in a recent experiment [11]. The one-dimensional model presented here falls short in explaining the 10 dB

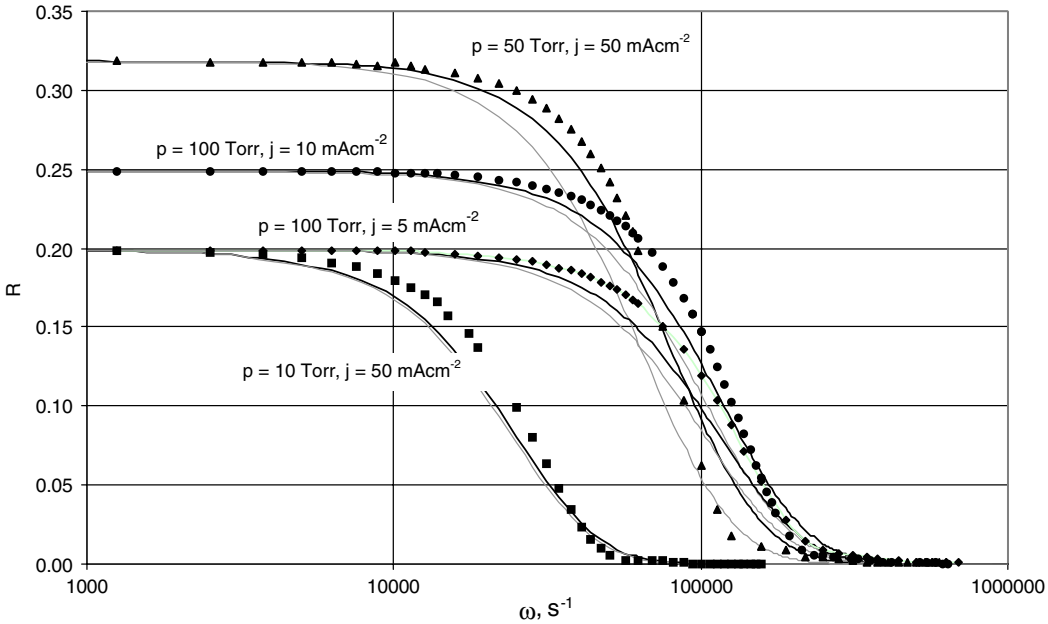

Figure 4. Coefficient of sound reflection from the gas-plasma boundary versus wave frequency, for different gas pressures, p, and discharge current densities, j, for temperature profiles that are shown in figure 5. Markers—numerical solution, dark and light lines—solutions given by equation (8) for the scattering integrals and least-square approximations, respectively.

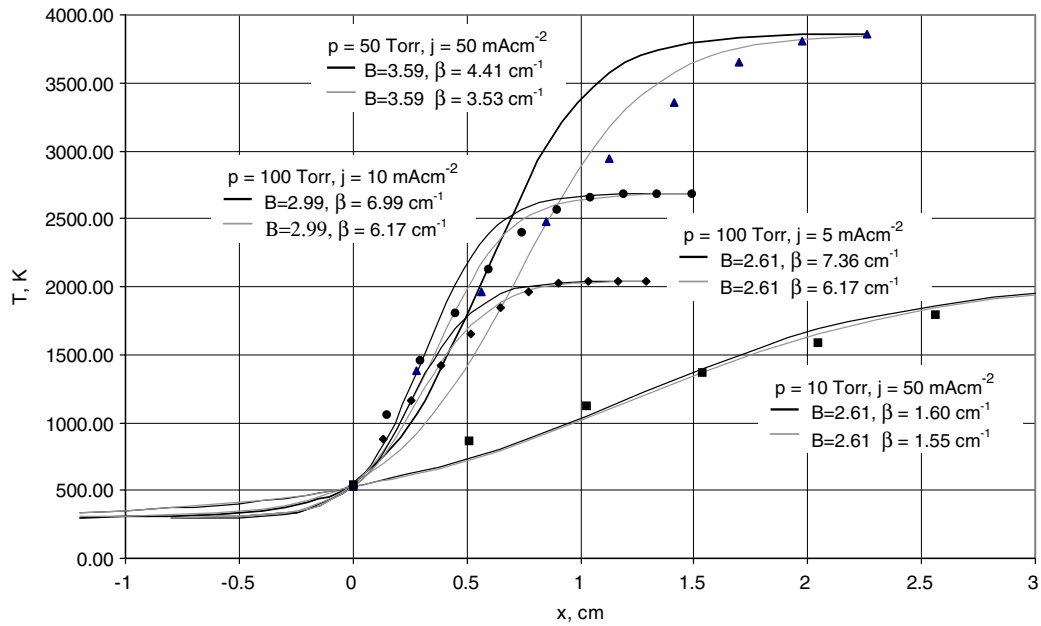

Figure 5. Gas temperature profiles in the gas–plasma boundary. Solid markers are numerical solutions for 'actual' temperature profiles calculated using the approach developed in [14]. The lines are model profiles given by equation (7). Parameters B and β are found using the fitting procedure based on the scattering integrals approach (darker lines) and by the least square method (lighter lines).

attenuation demonstrated in that experiment; however it provides sufficient evidence to suggest that the thermal gradient effect is a dominant mechanism in the attenuation of sound by a near-atmospheric glow discharge in air. The reflection coefficient increases with the angle of incidence, and, since the index of refraction of the cold air is greater than that for hot air, the angle of total internal refraction should exist. Therefore, the experimentally observed strong attenuation is most probably due to three-dimensional temperature gradient effects.

Appendix A. A solution for propagation of weak and strong acoustic waves in a non-uniform medium

The objective of this section is to develop an approach that governs propagation of an acoustic wave in an ideal gas where the pressure is constant throughout while the temperature and density distributions are non-uniform. Thermal conductivity and viscosity are not taken into account. In a non-uniform gas, the entropy is different at different locations. Here we consider the entropy constant on each particle path although the

entropy on different particle paths may have different values. With these approximations, the propagation of a wave in the non-uniform medium is described by Euler's equations:

$$\begin{aligned}&\frac{\partial\rho}{\partial t}+\nabla\cdot(\rho\vec{u})=0,\\&\frac{\partial\vec{u}}{\partial t}+(\vec{u}\cdot\vec{\nabla})\vec{u}+\frac{1}{\rho}\nabla p=0,\\&\frac{Ds}{Dt}=0.\end{aligned}\tag{A.1}$$

Here ρ, $\vec{u}$, p, s are the density, mass velocity, pressure and entropy of the gas, respectively.

Considering a one-dimensional case, we choose positive direction of the x-axis coinciding with mass velocity, $\vec{u}$. We choose mass velocity as an independent variable and make use of the following relations known for uniform media that could be proved valid for a non-uniform medium under consideration:

$$\frac{\partial\rho}{\partial u}=\pm\frac{\rho}{a},\tag{A.2}$$

$$\frac{\partial a}{\partial u}=\pm\frac{\gamma-1}{2}.\tag{A.3}$$

Introducing functions $\Phi(x,t)$ and $\mathrm{F}(x,t)$ which satisfy

$$a(u,x,t)=\Phi(x,t)\pm\frac{\gamma-1}{2}u\tag{A.4}$$

and

$$a(u,x,t)=F(x,t)\rho^{\frac{\gamma-1}{2}}(u,x,t)\tag{A.5}$$

and, using equations (A.3) and (A.4) that lead to

$$\frac{\partial^k\Phi}{\partial u^k}\equiv 0\frac{\partial^k F}{\partial u^k}\equiv 0\quad(k=0,1,2\ldots,)$$

the conservation equations can be reduced to

$$\begin{aligned}&\frac{\partial u}{\partial t}\pm(a\pm u)\frac{\partial u}{\partial x}=\mp\frac{2}{\gamma-1}\left\{\frac{\partial\Phi}{\partial t}+u\frac{\partial\Phi}{\partial x}\right\},\\&\frac{\partial\Phi}{\partial t}+u\frac{\partial\Phi}{\partial x}=\pm a\frac{\partial\Phi}{\partial x}\mp\frac{a^2}{\gamma}F\frac{\partial F}{\partial x},\\&\frac{\partial F}{\partial t}+u\frac{\partial F}{\partial x}=0.\end{aligned}\tag{A.6}$$

Since $\Phi(x,t)$ and $F(x,t)$ do not depend on u directly, linearization of equations of (A.6) should be done using a variational approach. A zero-order approximation (at $u=0$) is $\Phi|_{u=0}=a_0(x)$: $F|_{u=0}=a_0^{\gamma}(x)$. Representing the unknowns as

$$\begin{aligned}\Phi&=a_0(x)+\delta\Phi(x,t),\\F&=a_0^{\gamma}(x)+\delta F(x,t),\end{aligned}\tag{A.7}$$

where $\delta\Phi,\delta F$ are small perturbations, substituting (A.7) with (A.6) and neglecting higher-order terms one can obtain, consecutively accounting for linear, quadratic and higher-order terms, equation (1) for linear waves as well as equations for non-linear waves.

References

[1] Klimov A I *et al* 1982 *Sov. Phys. Tech. Phys.* **8** 146
[2] Mishin G I 1985 *Sov. Tech. Phys. Lett.* **11** 112
[3] Mishin G I, Serov Yu L and Yavor I P 1991 *Sov. Tech. Phys. Lett.* **17** 413
[4] Ganguly B N, Bletzinger P and Garscadden A 1998 *Phys. Lett.* A **230** 218
[5] Soukhomlinov V S *et al* 2002 *J. Fluid Mech.* **473** 245
[6] Macheret S *et al* 2001 *Phys. Fluids* **13** 2693
[7] Soukhomlinov V S *et al* 2002 *Phys. Fluids* **14** 427
[8] Roth J R, Sherman D M and Wilkinson S P 2000 *AIAA J.* **38** 1166
[9] Girgis I G, Schneider M N, Macheret S O, Brown G L and Miles R B 2002 Creation of steering moments in a supersonic flow by off-axis plasma heat addition *Proc. 4th AIAA Aerospace Sciences Meeting (Reno, NV, 14–17 January 2002)*
[10] Corke T C, Jumper E J, Port M L and Orlov D 2002 Application of weakly ionized plasmas as wing flow-control devices *Proc. 4th AIAA Aerospace Sciences Meeting (Reno, NV, 14–17 January 2002)*
[11] Stepaniuk V *et al* 2004 *AIAA J.* **42** 454
[12] Strutt J W (Baron Rayleigh) 1945 *Theory of Sound* (New York: Dover) vol 2 pp 78–88
[13] Whitham G B 1974 *Linear and Nonlinear Waves* (New York: Wiley) p 622
[14] Soukhomlinov V S, Sheverev V A and Ötügen V M 2003 *J. Appl. Phys.* **94** 844
[15] Gridin A Yu, Klimov A I and Molevich N E 1993 *Sov. Phys. Tech. Phys.* **63** 158
[16] Landau L and Lifshitz E 1977 *Quantum Mechanics* (Oxford: Pergamon) pp 76–81.
[17] Froman N and Froman P O 1965 *JWKB Approximation* (Sweden: Institute of Theoretical Physics, University of Uppsala) p 168
[18] Hecht C E and Mayer J E 1957 *Phys. Rev.* **106** 1156
[19] Tannehill J C, Anderson D A and Pletcher R H 1997 *Computational Fluid Mechanics and Heat Transfer* (London: Taylor and Francis) p 792